

## Recognition and Processing of a New Repertoire of DNA Substrates by Human 3-Methyladenine DNA Glycosylase (AAG)<sup>†</sup>

Chun-Yue I. Lee,<sup>‡,§</sup> James C. Delaney,<sup>§,||,⊥</sup> Maria Kartalou,<sup>§,||</sup> Gondichatnahalli M. Lingaraju,<sup>§,||</sup>  
Ayelet Maor-Shoshani,<sup>§,||</sup> John M. Essigmann,<sup>§,||,⊥</sup> and Leona D. Samson<sup>\*,§,||,+</sup>

Department of Chemical Engineering, Center for Environmental Health Sciences, Department of Biological Engineering,  
Department of Chemistry, and Department of Biology, Massachusetts Institute of Technology, Cambridge, Massachusetts 02139

Received October 7, 2008; Revised Manuscript Received January 5, 2009

**ABSTRACT:** The human 3-methyladenine DNA glycosylase (AAG) recognizes and excises a broad range of purines damaged by alkylation and oxidative damage, including 3-methyladenine, 7-methylguanine, hypoxanthine (Hx), and 1,*N*<sup>6</sup>-ethenoadenine ( $\epsilon$ A). The crystal structures of AAG bound to  $\epsilon$ A have provided insights into the structural basis for substrate recognition, base excision, and exclusion of normal purines and pyrimidines from its substrate recognition pocket. In this study, we explore the substrate specificity of full-length and truncated  $\Delta$ 80AAG on a library of oligonucleotides containing structurally diverse base modifications. Substrate binding and base excision kinetics of AAG with 13 damaged oligonucleotides were examined. We found that AAG bound to a wide variety of purine and pyrimidine lesions but excised only a few of them. Single-turnover excision kinetics showed that in addition to the well-known  $\epsilon$ A and Hx substrates, 1-methylguanine (m1G) was also excised efficiently by AAG. Thus, along with  $\epsilon$ A and ethanoadenine (EA), m1G is another substrate that is shared between AAG and the direct repair protein AlkB. In addition, we found that both the full-length and truncated AAG excised 1,*N*<sup>2</sup>-ethenoguanine (1,*N*<sup>2</sup>- $\epsilon$ G), albeit weakly, from duplex DNA. Uracil was excised from both single- and double-stranded DNA, but only by full-length AAG, indicating that the N-terminus of AAG may influence glycosylase activity for some substrates. Although AAG has been primarily shown to act on double-stranded DNA, AAG excised both  $\epsilon$ A and Hx from single-stranded DNA, suggesting the possible significance of repair of these frequent lesions in single-stranded DNA transiently generated during replication and transcription.

DNA-damaging agents are ubiquitous, and cellular DNA is constantly attacked by a variety of endogenous and exogenous DNA-damaging agents. DNA can be deaminated spontaneously or alkylated by endogenous intracellular sources and by exogenous environmental agents. Such damages can interfere with DNA replication and transcription and may be mutagenic or cytotoxic to the cell. During evolution, multiple DNA repair pathways have evolved to maintain the integrity of DNA in all organisms. Among other pathways, single-base aberrations can be repaired by the base excision repair (BER) pathway. BER is initiated by DNA glycosylases that recognize the damaged base in the genome, followed by hydrolysis of the *N*-glycosylic bond, resulting in the release of the damaged base and the generation of an

abasic site. The abasic site is further processed by an AP<sup>1</sup> endonuclease or AP lyase, resulting in a strand break. After trimming of the DNA ends, DNA is resynthesized by a DNA polymerase and a DNA ligase seals the nick to restore undamaged DNA (1).

Many DNA glycosylases exhibit strict substrate specificity. The human 3-methyladenine DNA glycosylase (AAG), by contrast, is able to recognize and excise structurally diverse bases, including 3-methyladenine, 7-methylguanine, 1-*N*<sup>6</sup>-ethenoadenine ( $\epsilon$ A), and hypoxanthine (Hx), from DNA (2–8). The crystal structure of AAG bound to DNA containing  $\epsilon$ A provides insight into the binding and catalysis by this DNA

<sup>†</sup> This work was supported by NIH Grants ES05355, CA75576, CA55042, ES02109, T32-ES007020, CA80024, and CA26731, and L.D.S. is an American Cancer Society Research Professor.

\* To whom correspondence should be addressed. Phone: (617) 258-7813. Fax: (617) 253-8099. E-mail: lsamson@mit.edu.

<sup>‡</sup> Department of Chemical Engineering.

<sup>§</sup> Center for Environmental Health Sciences.

<sup>||</sup> Department of Biological Engineering.

<sup>⊥</sup> Department of Chemistry.

<sup>+</sup> Department of Biology.

<sup>1</sup> Abbreviations: AAG, human 3-methyladenine DNA glycosylase; m1G, 1-methylguanine; m1A, 1-methyladenine; m3T, 3-methylthymine; m3C, 3-methylcytosine; m3U, 3-methyluracil; e3U, 3-ethyluracil; EA, 1,*N*<sup>6</sup>-ethanoadenine;  $\epsilon$ A, 1,*N*<sup>6</sup>-ethenoadenine;  $\epsilon$ C, 3,*N*<sup>4</sup>-ethenocytosine; 1,*N*<sup>2</sup>- $\epsilon$ G, 1,*N*<sup>2</sup>-ethenoguanine; M1G, pyrimido[1,2- $\alpha$ ]purin-10(3*H*)-one; Hx, hypoxanthine; U, uracil; AP, apurinic; ABH, AlkB homologue; BCNU, 1,3-bis(2-chloroethyl)-1-nitrosourea; EDTA, ethylenediamine-tetraacetic acid; EGTA, ethylene glycol bis(2-aminoethyl ether)-*N,N,N',N'*-tetraacetic acid; BSA, bovine serum albumin; AlkB, *Escherichia coli* 3-methyladenine DNA glycosylase; UDG, uracil DNA glycosylase; UNG2, nuclear uracil DNA glycosylase; SMUG1, single-strand-selective monofunctional uracil-DNA glycosylase 1; SD, standard deviation.

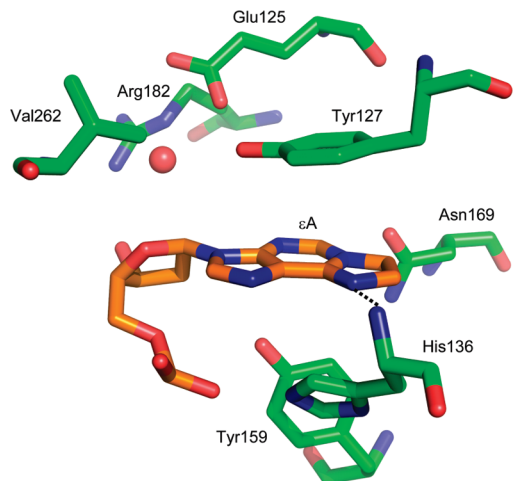


FIGURE 1: Structure of the AAG active site (green) showing the flipped-out  $\epsilon$ A nucleotide (gold). The dashed line indicates a hydrogen bond between N6 of  $\epsilon$ A (acceptor) and the peptide amide (donor) of His136. This figure was generated using the coordinates of the AAG- $\epsilon$ A crystal structure [Protein Data Bank entry 1f4r (9)] using Pymol.

glycosylase (Figure 1) (9). In the active site complex, the substrate nucleotide is rotated in the plane of the base pair out of the duplex DNA into the active site of the enzyme. Tyr162 of the enzyme is intercalated into the space vacated by the lesion via the DNA minor groove, maintaining proper base stacking and minimizing DNA distortion (9, 10). A water molecule is involved in the nucleophilic attack on the *N*-glycosylic bond by an acid–base catalytic mechanism with Glu125 acting as a general base (9–11). Equally important, the discrimination against pyrimidines is likely due to the fact that AAG employs an acid–base catalysis that is more suitable for selective excision of purines (11). In addition, the possible steric clash of the Asn169 side chain with the 2-amino group of guanine and the inability of the 6-amino group of adenine to accept a hydrogen bond from His136 may exclude these undamaged purine bases from the binding pocket (9, 12).

In contrast to AAG, AlkB is an orthogonal DNA repair protein that can directly reverse alkylation damage catalytically. *Escherichia coli* AlkB had first been shown to repair methylated lesions, such as 1-methyladenine (m1A) and 3-methylcytosine (m3C), in DNA and RNA (13, 14) via oxidative demethylation. Subsequently, 1-methylguanine (m1G) (15, 16), 3-methylthymine (m3T) (15–17), and 3-ethylcytosine (15) were also found to be AlkB substrates, although with weaker activity on m1G and m3T than on m1A and m3C. Among the human AlkB homologues discovered thus far, only hABH1, hABH2, and hABH3 have been shown to have repair activity on DNA and also RNA (14, 18–21). In addition to simple methylated base adducts, AlkB was recently shown in *E. coli* and in vitro studies to repair 1,*N*<sup>6</sup>-ethanoadenine (EA) (22),  $\epsilon$ A (23, 24), and 3,*N*<sup>4</sup>-ethenocytosine ( $\epsilon$ C) (23). In vivo (in mouse) and in vitro repair activity on  $\epsilon$ A has been shown for mammalian ABH2 (25).

Although *E. coli* AlkB and the human ABH proteins are able to repair etheno lesions, the mechanism of their repair is completely different from AAG-initiated BER, which also repairs  $\epsilon$ A and EA DNA lesions. Etheno base lesions can be formed endogenously by the products of lipid peroxidation and can be induced by exposure to environmental sources

such as vinyl chloride and its metabolites chloroethylene oxide and chloroacetaldehyde (26–33). EA is similar to  $\epsilon$ A with the exception of having a saturated C–C bond in place of the double bond between the two exocyclic carbon atoms bridging the *N*<sup>6</sup> exocyclic and *N*1 heterocyclic nitrogens of adenine. EA can be formed from the reaction between DNA and 1,3-bis(2-chloroethyl)-1-nitrosourea (BCNU) (34), a chemotherapeutic agent commonly used to treat brain tumors; EA can be repaired by AAG, albeit inefficiently (35). Having two different mechanisms for the repair of such an important class of lesions could be advantageous, and the relative activities of each pathway may differ between tissue and cell types.

In this study, we have tested the binding and glycosylase activity of AAG against a library of lesion-containing DNA oligonucleotides (Figure 2) and have identified new substrates for AAG. Both the full-length version and a truncated version of AAG missing the 80 N-terminal amino acids ( $\Delta$ 80AAG) were used in this study, whereas previous studies primarily focused on truncated AAG, because it is more easily purified. We have shown that m1G, in addition to the already-known substrates  $\epsilon$ A and EA, is a substrate shared between AAG and AlkB. On the basis of earlier work showing that  $\epsilon$ A and Hx are refractory to repair when situated opposite a reduced abasic site (36), it was thought that excision is only possible in double-stranded (ds) DNA. However, in this study it was surprising to find that both the truncated and full-length AAG can excise  $\epsilon$ A and Hx from single-stranded (ss) DNA. Furthermore, we found that both full-length AAG and  $\Delta$ 80AAG have weak glycosylase activity on 1,*N*<sup>2</sup>- $\epsilon$ G. Finally, we found that only full-length AAG, but not  $\Delta$ 80AAG, excises uracil in both ss- and ds-DNA. We demonstrate here, using a library of lesion-containing single- and double-stranded DNA oligonucleotides, that AAG has a wide range of substrate specificity, including multiple classes of new substrates.

## EXPERIMENTAL PROCEDURES

**DNA Oligonucleotides.** Oligonucleotides containing m1G, m1A, m3T, and m3C were synthesized as described by Delaney and Essigmann (15). The synthesis of the oligonucleotide containing EA was described by Frick et al. (22), of those containing  $\epsilon$ A and  $\epsilon$ C by Delaney et al. (23), of those containing 1,*N*<sup>2</sup>- $\epsilon$ G by Goodenough et al. (37), and of those containing M1G by Wang et al. (38), and the synthesis of oligonucleotides containing m3U and e3U will be published elsewhere. Oligonucleotides containing Hx and U were synthesized using phosphoramidites from Glen Research (Sterling, VA). All of the oligonucleotides were 16-mers with identical sequence (5′GAAGACCTXGGCGTCC3′) where the only difference is in the central lesion, X (Figure 2). The single-stranded oligonucleotides were 5′-end-labeled with <sup>32</sup>P and purified using a MicroSpin G-25 column (GE Healthcare). For studies involving double-stranded DNA substrates, annealing was performed using a 1:1.5 ratio of modified to unlabeled complement. The base opposite the lesion was chosen to be the natural base-pairing partner of the undamaged base. For U, m3U, and e3U, guanine was used as the opposing base, since the lesions here were assumed to form from deamination of cytosine and 3-alkylcytosine.

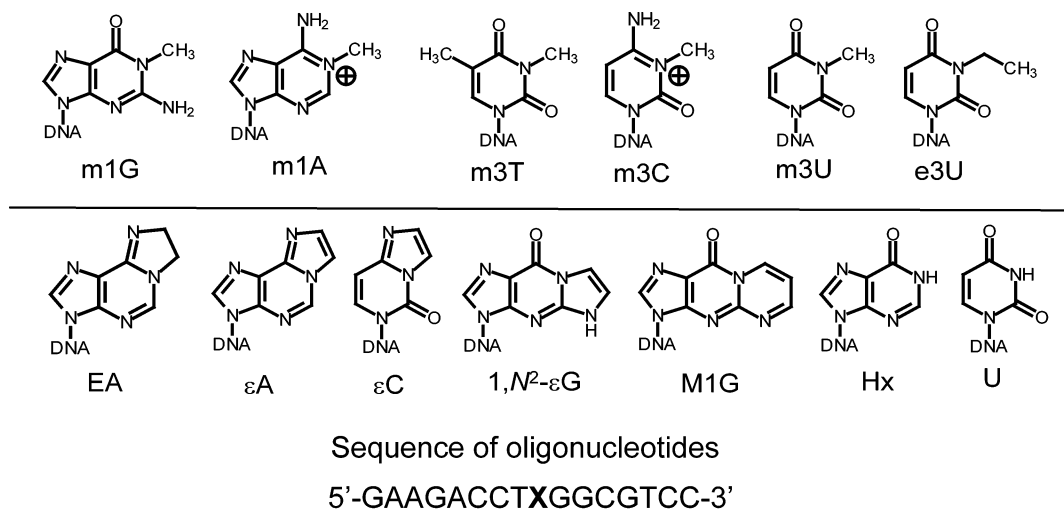


FIGURE 2: Chemical structures and sequence context of the different DNA lesions tested in this study.

**AAG Protein Expression and Purification.**  $\Delta 80$ AAG with the first 80 amino acids deleted from the N-terminus and the full-length AAG protein were both used in this study. The  $\Delta 80$ AAG and full-length AAG proteins were cloned and purified as described previously (11) with and without the gel filtration step, respectively. Previous studies have shown that AAG possessing a truncation of its N-terminal domain has catalytic activity similar to that of the full-length protein (6, 11).

**DNA Glycosylase Activity Assays.** Glycosylase assays were performed by incubation of 1000 nM AAG protein (10 pmol) and 10 nM  $^{32}$ P-labeled DNA substrate (100 fmol) at 37 °C in 10  $\mu$ L of assay buffer containing 20 mM Tris-HCl buffer (pH 7.8), 100 mM KCl, 5 mM  $\beta$ -mercaptoethanol, 2 mM EDTA, 1 mM EGTA, and 50  $\mu$ g/mL BSA. The experiments were carried out under single-turnover conditions where the enzyme concentration was in 100-fold excess of the labeled DNA substrate concentration. Initial screening experiments of AAG glycosylase activity were performed by incubating a 1:100 molar ratio of DNA oligonucleotide to AAG enzyme in glycosylase buffer for 90 min (or 180 min for 1,N<sup>2</sup>- $\epsilon$ G and uracil). For subsequent kinetics experiments, an aliquot of the reaction mixture was removed for quenching at various time points during the course of the incubation. Reactions were quenched with 0.2 N NaOH, except for  $\epsilon$ C and m3C where 0.2 M piperidine was used, and then mixtures were heated at 75 °C for 15 min to cleave the DNA at AP sites. Samples were then diluted with formamide loading buffer, and cleavage products were resolved on a 20% denaturing polyacrylamide gel. The fraction of uncleaved versus cleaved substrate was determined on a Packard Cyclone PhosphorImager (Packard Instruments, Meriden, CT), analyzed with OptiQuant (Packard Instruments), and quantified with the Kodak 1D scientific imaging software (Eastman Kodak Co., New Haven, CT). Enzymatic rate constants were determined by fitting the single-turnover kinetic data into the One Phase Exponential Association equation (eq 1) using GraphPad Prism (GraphPad Software, Inc., La Jolla, CA):

$$y = y_{\max}(1 - e^{-k_{\text{obs}}t}) \quad (1)$$

where  $y$  is the amount of substrate cleaved at any particular time point,  $y_{\max}$  is the maximum amount of cleaved substrate,  $t$  is time, and  $k_{\text{obs}}$  is the observed rate constant. Rate constants

for extremely slow reactions where the increase in cleaved substrate amount did not follow an exponential increase were determined using linear regression in the form of  $y = k_{\text{obs}}t$ .

**Electrophoretic Mobility Shift (Gel Shift) Assays (EMSAs).** Binding assays were performed in an assay buffer containing 50 mM HEPES (pH 7.5), 100 mM NaCl, 5 mM  $\beta$ -mercaptoethanol, 9.5% (v/v) glycerol, and 0.1 mg/mL BSA.  $^{32}$ P-labeled DNA substrate (2 nM) was incubated with increasing concentrations of AAG in the binding assay buffer for 30 min at 4 °C and then directly loaded onto a 6% nondenaturing polyacrylamide gel. After electrophoresis, the gel was dried and the fraction of DNA bound by AAG was analyzed and quantified as described above for the glycosylase assays. The apparent dissociation constant  $K_d$  was calculated by fitting the quantified binding data to the One Site Binding (hyperbola) equation (eq 2) in GraphPad Prism (GraphPad Software, Inc.).

$$y = \frac{B_{\max}x}{K_d + x} \quad (2)$$

where  $y$  is the total amount of bound substrate,  $B_{\max}$  is the maximum specific binding,  $x$  is the concentration of the protein, and  $K_d$  is the apparent binding constant.

## RESULTS

**AAG Recognizes a Wide Range of DNA Lesions.** To investigate thoroughly the substrate specificity of AAG, a wide range of lesion-containing DNA oligonucleotides was interrogated (Figure 2). Substrate binding and glycosylase activity of both the full-length and  $\Delta 80$ AAG proteins were measured for single- and double-stranded lesion-containing DNA oligonucleotides. Their identical sequence context allowed us to eliminate the possible effects resulting from the flanking base sequence on the ability of AAG to bind and excise. Lesion recognition and substrate binding were assessed by gel shift assays. To determine the quantitative binding affinity of AAG for the base lesions, shown in Figure 2, various concentrations of AAG were incubated with a fixed amount of substrate in duplex DNA. Surprisingly, AAG was found to bind a large number of lesions in duplex DNA, but to different extents (Table 1). It is important to note that for all the lesions tested, band shifts were observed only using



Table 1: Binding and Excision Kinetic Constants of Various Lesions by AAG<sup>a</sup>

base excised:pairing partner	binding	glycosylase activity				
	$\Delta 80\text{AAG}$	$\Delta 80\text{AAG}$		full-length AAG		
	$K_d \pm \text{SD (nM)}$	$k_{\text{obs}} \pm \text{SD (min}^{-1}\text{)}^b$	initial excision rate (fmol/min) <sup>c</sup>	$k_{\text{obs}} \pm \text{SD (min}^{-1}\text{)}^b$	$k_{\text{obs}} \pm \text{SD (fmol/min)}^d$	initial excision rate (fmol/min) <sup>c</sup>
m1G:C	648 $\pm$ 154	0.101 $\pm$ 0.010	4.46	0.065 $\pm$ 0.005		3.68
m1A:T	176 $\pm$ 28	NA	NA	NA		NA
m3T:A	189 $\pm$ 35	NA	NA	NA		NA
m3C:G	61 $\pm$ 9	NA	NA	NA		NA
m3U:G	27 $\pm$ 4	NA	NA	NA		NA
e3U:G	103 $\pm$ 12	NA	NA	NA		NA
$\epsilon\text{A:T}$	7 $\pm$ 1	0.027 $\pm$ 0.003	1.98	0.029 $\pm$ 0.003		2.12
EA:T	340 $\pm$ 129	0.017 $\pm$ 0.001	0.47	0.016 $\pm$ 0.001		0.51
$\epsilon\text{C:G}$	10 $\pm$ 1	NA	NA	NA		NA
1,N <sup>2</sup> - $\epsilon\text{G:C}$	928 $\pm$ 137	0.079 $\pm$ 0.011	0.44	0.074 $\pm$ 0.012		0.46
M1G:C	NB	NA	NA	NA		NA
Hx:T	125 $\pm$ 30	0.425 $\pm$ 0.070	30.4	0.390 $\pm$ 0.061		27.6
U:G	NB	NA	NA		0.062 $\pm$ 0.002 <sup>d</sup>	0.062 <sup>d</sup>
$\epsilon\text{A (ss)}$	NB	0.030 $\pm$ 0.006	1.22	0.043 $\pm$ 0.005		1.65
Hx (ss)	NB	0.062 $\pm$ 0.011	2.01	0.061 $\pm$ 0.007		1.90
U (ss)	NB	NA	NA		0.063 $\pm$ 0.003 <sup>d</sup>	0.063 <sup>d</sup>

<sup>a</sup> Full-length AAG was not observed to bind DNA at all in the gel shift assay.  $\Delta 80\text{AAG}$  was not observed to bind to single-stranded DNA. NB and NA represent no detectable binding and no activity, respectively ( $<0.3\%$  and 0.3 fmol, respectively). <sup>b</sup> Activity rate constants  $k_{\text{obs}}$  were determined from one-phase exponential association except for U. <sup>c</sup> The initial rate is the product of the rate constant  $k_{\text{obs}}$  and the maximum saturation cleavage (maximum amount of abasic product formed), except for U where the initial rate is equal to the rate constant obtained from linear regression. <sup>d</sup> Rate data for U were fitted with linear regression in the form of  $y = kt$ .

the truncated  $\Delta 80\text{AAG}$  and not the full-length protein (data not shown). However, the factors responsible for not observing band shifts with the full-length AAG are presently unknown. Hence, only the binding data for  $\Delta 80\text{AAG}$  are shown. However, using surface plasmon resonance, full-length AAG has been shown to bind to DNA oligonucleotides containing Hx and AP sites (39).

Figure 3 shows representative experiments for a weak binding substrate (m1G), a moderate binding substrate (e3U), and a very strong binding substrate ( $\epsilon\text{A}$ ) with  $\Delta 80\text{AAG}$  (Figure 3A,C,E), with corresponding quantification of the binding (Figure 3B,D,F), from which the apparent dissociation constants ( $K_d$ ) were calculated (Table 1). The strongest affinity was observed for  $\epsilon\text{A}$  and  $\epsilon\text{C}$ , with a  $K_d$  of  $\sim 10$  nM, followed by m3U with a  $K_d$  of  $\sim 30$  nM. AAG exhibited moderate binding affinity for m3C, Hx, e3U, m1A, and m3T, with apparent binding constants between 60 and 200 nM. Weak to very weak binding was observed for EA ( $K_d = 340$  nM), m1G ( $K_d = 648$  nM), and 1,N<sup>2</sup>- $\epsilon\text{G}$  ( $K_d = 928$  nM). AAG bound several AlkB substrates; these include simple methylated bases (m1G, m1A, m3T, and m3C), as well as the more complex cyclic lesions EA,  $\epsilon\text{A}$ , and  $\epsilon\text{C}$ . The apparent relative strength of AAG binding was as follows:  $\epsilon\text{A}$  and  $\epsilon\text{C} > \text{m3C} > \text{m1A} > \text{m3T} > \text{EA} > \text{m1G}$  (Table 1).

It is also interesting to note that, in addition to  $\epsilon\text{A}$  and  $\epsilon\text{C}$ , AAG exhibited very strong binding to 3-methyluracil (m3U) and 3-ethyluracil (e3U), but not to uracil itself. Very weak binding for 1,N<sup>2</sup>- $\epsilon\text{G}$  was seen, but no binding was detected for M1G. In a comparison of the difference in binding affinity of U, m3U, and m3T in relation to their structural similarity, m3U differs from U by the addition of a methyl group at the N3 position, yet this modification is sufficient to increase its binding affinity for AAG significantly to a  $K_d$  of  $\sim 30$  nM compared with no binding shown by U. However, the binding affinity of m3T ( $K_d \sim 200$  nM), which has methyl groups on both N3 and C5 analogous positions of uracil, was much lower than that of m3U.

#### AAG Excises Only a Few of the Lesions to Which It Binds.

We tested the glycosylase activity for both the full-length protein and  $\Delta 80\text{AAG}$  on the library of lesion-containing oligonucleotides. The glycosylase reactions were carried out under single-turnover conditions where the enzyme was in 100-fold molar excess of the oligonucleotide substrate, such that the reaction kinetics should not be a function of enzyme–substrate binding rates (12). Single-turnover glycosylase kinetics measures the rate of reaction steps after formation of the initial AAG–DNA complex (12).

Single-turnover glycosylase activity assays were performed with time courses of up to 90 or 180 min, depending on the reaction rates. Among the damaged bases tested, AAG was active on m1G, EA,  $\epsilon\text{A}$ , Hx, 1,N<sup>2</sup>- $\epsilon\text{G}$ , and uracil in double-stranded DNA; AAG was also active on  $\epsilon\text{A}$ , Hx, and uracil in single-stranded DNA (Table 1). Both full-length and truncated AAG appeared to exhibit very similar excision kinetics for most substrates except for U. No glycosylase activity was observed toward m1A, m3T, m3C, m3U, e3U,  $\epsilon\text{C}$ , or M1G (Table 1). Among the various AlkB substrates tested (m1G, m1A, m3T, m3C, EA,  $\epsilon\text{A}$ , and  $\epsilon\text{C}$ ), AAG-mediated excision was observed only for m1G, EA, and  $\epsilon\text{A}$ . Thus, among the methylated AlkB substrates, m1G was the only lesion to be repaired by AAG, with a fairly fast observed rate constant of  $\sim 0.1 \text{ min}^{-1}$  for both the full-length protein and  $\Delta 80\text{AAG}$  (Figure 4A,B and Table 1). It is interesting that despite AAG's ability to bind to all four methylated lesions, only m1G was excised, even though AAG bound m1G the least tightly among the four (Table 1). Although the purine site of alkylation for m1G is identical to m1A, AAG did not excise m1A (Table 1). m3T and m3C are pyrimidines and are not expected to be excised by AAG on the basis of the acid–base catalytic mechanism that favors the removal of damaged purines (11). Two other AlkB substrates repaired by AAG were EA and  $\epsilon\text{A}$  in duplex DNA. Guliaev et al. (35) previously reported that EA is a 65-fold weaker substrate for AAG than  $\epsilon\text{A}$ ; however, this study

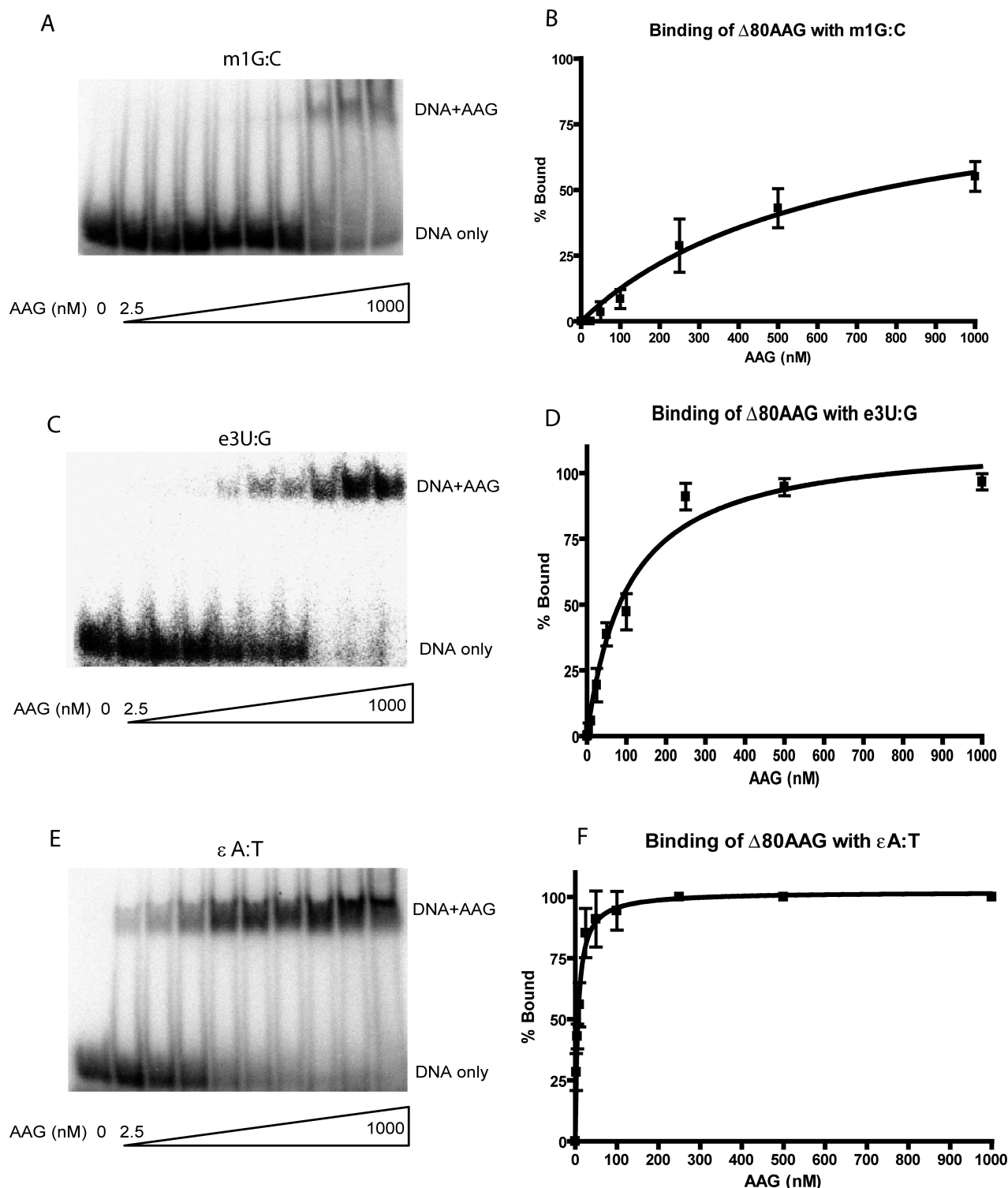


FIGURE 3:  $\Delta 80$ AAG binds to different lesions with different affinities. Gel mobility shift assay for the binding of  $\Delta 80$ AAG to oligonucleotides containing (A) m1G, (C) e3U, and (E)  $\epsilon$ A. Graphical representation of the binding of  $\Delta 80$ AAG to (B) m1G, (D) e3U, and (F)  $\epsilon$ A.

shows the excision rates of EA and  $\epsilon$ A to be far less disparate with initial rates of 0.5 and 2.0 fmol/min, respectively (Figures 4C,D and 5A,B and Table 1). No glycosylase activity toward  $\epsilon$ C was observed despite AAG's very strong binding affinity for this lesion (Table 1).

*Single-Turnover Kinetics of Excision of 1,N<sup>6</sup>-Ethenoadenine and Hypoxanthine from Single- and Double-Stranded DNA.* The activity of AAG on  $\epsilon$ A and Hx substrates was measured to compare its excision activity on newly identified substrates in the same sequence context; excision kinetics

for  $\Delta 80$ AAG and full-length AAG were monitored for up to 90 min (Figure 5). The observed rate constant for the  $\epsilon$ A:T pair was found to be  $\sim 0.03 \text{ min}^{-1}$  for both full-length and  $\Delta 80$ AAG (Table 1), and those for the Hx:T pair were  $\sim 0.4 \text{ min}^{-1}$  (Table 1); therefore, the excision rates for these lesions do not appear to be influenced by truncation of AAG's N-terminus.

We unexpectedly also saw that AAG exhibited catalytic activity against  $\epsilon$ A and Hx in single-stranded DNA (Figure 5A,C,D,F). Although most previous studies have monitored

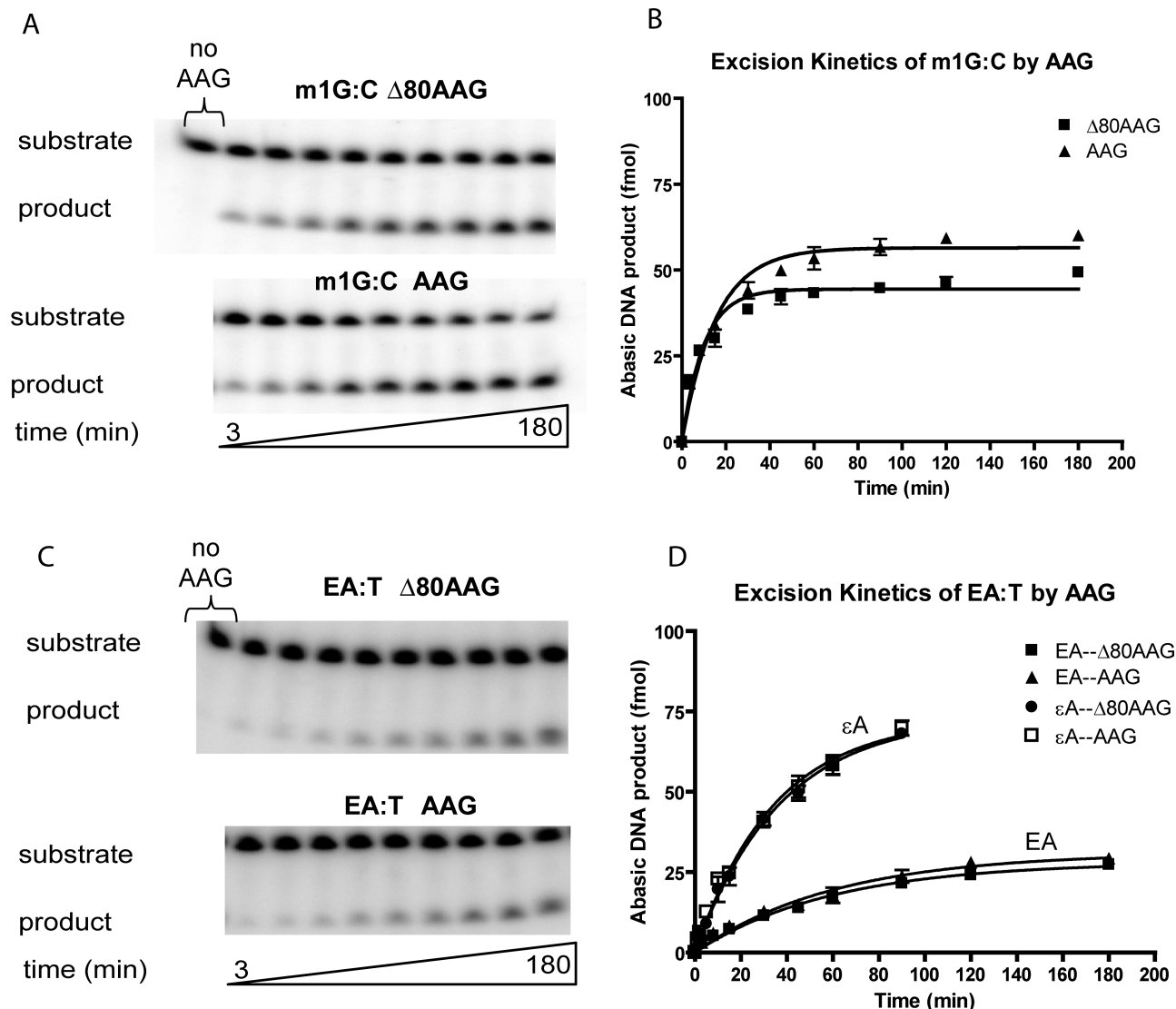


FIGURE 4: m1G and EA, known AlkB substrates, are cleaved by AAG when present in double-stranded DNA. Glycosylase activity of AAG toward (A) m1G and (C) EA. No AAG represents incubation without AAG for the longest time point of the assay. Graphical representation of the glycosylase activity toward (B) m1G and (D) EA by (■) Δ80AAG and (▲) full-length AAG. For comparison with EA, the data of AAG glycosylase activity toward εA from Figure 5B are also shown in panel D: (●) Δ80AAG and (□) full-length AAG.

AAG activity on duplex DNA, activity on single-stranded DNA was previously reported for oxanine and εA (40). Among all adducts tested in this study, the only substrates that could be excised from single-stranded DNA by AAG were εA and Hx (and uracil, which was weakly excised). Interestingly, the observed rate constants for εA in single- and double-stranded DNA were very similar ( $\sim 0.03$ – $0.04 \text{ min}^{-1}$ ) (Table 1), and the initial excision rates were only slightly higher ( $\sim 1.5$ -fold) for duplex DNA than for single-stranded DNA (Table 1). In contrast, the observed rate constants and initial excision rates for Hx in single-stranded DNA ( $\sim 0.06 \text{ min}^{-1}$  and  $2 \text{ fmol/min}$ , respectively) were  $\sim 7$ - and  $15$ -fold lower, respectively, than those in duplex DNA ( $\sim 0.4 \text{ min}^{-1}$  and  $30 \text{ fmol/min}$ , respectively) (Table 1).

**Both Δ80AAG and Full-Length AAG Excise  $1,N^2$ -εG.** It was previously shown that glycosylase activity toward  $1,N^2$ -εG in duplex DNA was observed for full-length AAG, but not for the truncated form of AAG lacking the first 73 amino acids (41). It was also shown that the inability to excise was not due to an inability to bind, since the truncated AAG was observed to bind  $1,N^2$ -εG (41); thus, it was concluded that

the nonconserved, N-terminal part of AAG was essential for glycosylase activity toward  $1,N^2$ -εG (41). However, here we show that both Δ80AAG and full-length AAG were able to cleave  $1,N^2$ -εG from double-stranded DNA, albeit to a limited extent. As seen from Figure 6, both forms of the protein excised  $\sim 6\%$  of the  $1,N^2$ -εG base lesion at saturation, with observed rate constants of  $0.08$  and  $0.07 \text{ min}^{-1}$  for Δ80AAG and full-length AAG, respectively (and initial rates of  $\sim 0.5 \text{ fmol/min}$ ) (Table 1). Such rate constants were among the third highest of the lesions tested in this study, while the corresponding initial excision rates turned out to be very low. However, neither AAG glycosylase activity nor binding was observed for the structurally similar M1G adduct (Figure 2 and Table 1).

**Excision of Uracil from Single- and Double-Stranded DNA by AAG.** In addition to hypoxanthine (the deamination product of adenine), AAG has also been shown to excise the guanine-derived deaminated bases xanthine (42) and oxanine (40). Here, we observed that deaminated cytosine, namely uracil (U), was excised by AAG, although very slowly (Figure 7 and Table 1). Moreover, like oxanine, U

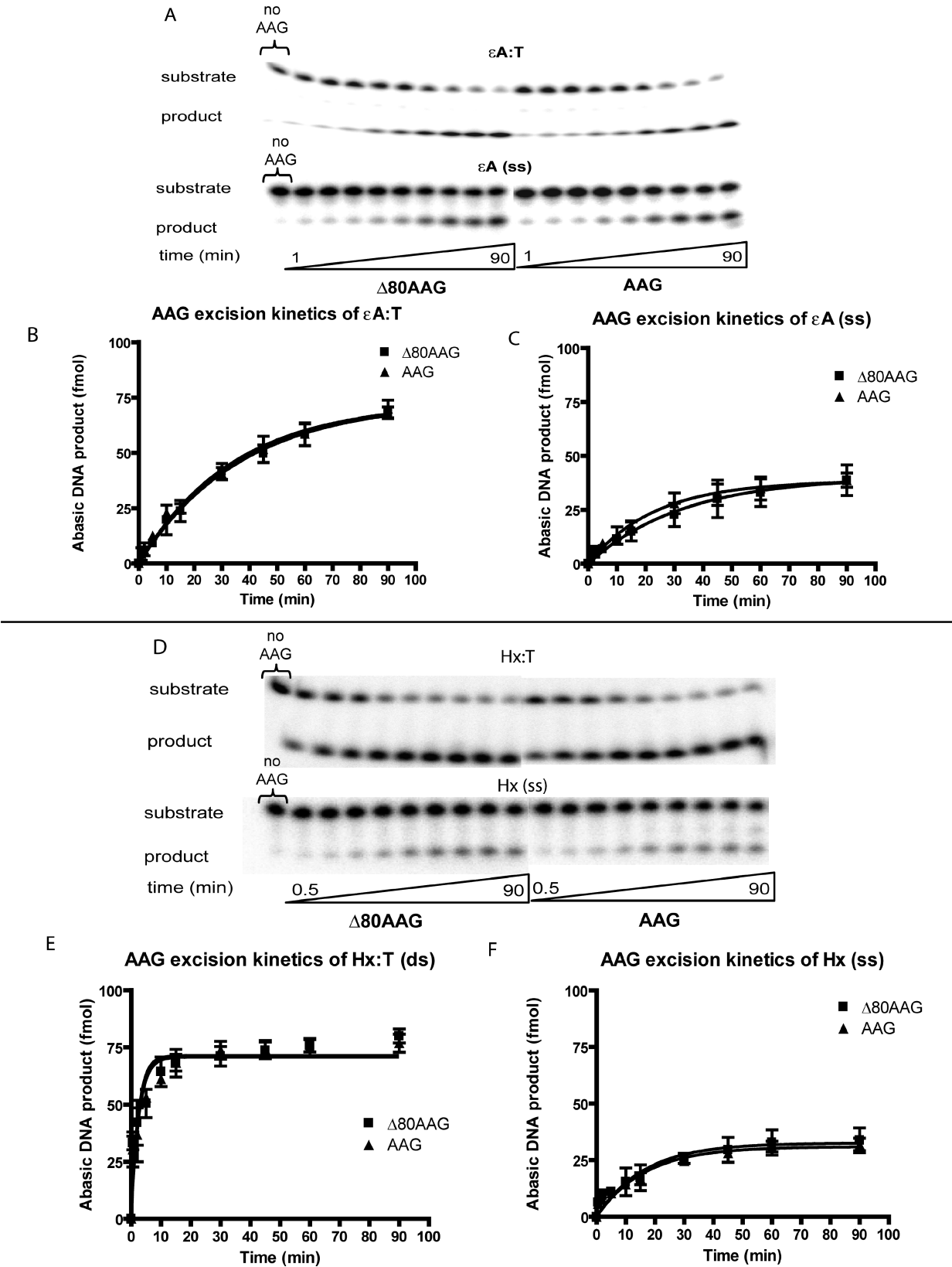


FIGURE 5: AAG cleaves  $\epsilon A$  and Hx in both double-stranded and single-stranded DNA. Glycosylase activity of AAG toward  $\epsilon A$  and Hx. Gels showing AAG excision of  $\epsilon A$  in (A) double- and single-stranded DNA. No AAG represents incubation without AAG for the longest time point of the assay. Graphical representation of the glycosylase activity toward  $\epsilon A$  in (B) duplex DNA and (C) single-stranded DNA by (■)  $\Delta 80AAG$  and (▲) full-length AAG. Gels showing excision of Hx in (D) double- and single-stranded DNA. No AAG represents incubation without AAG for the longest time point of the assay. Graphical representation of the glycosylase activity toward Hx in (E) duplex and (F) single-stranded DNA by (■)  $\Delta 80AAG$  and (▲) full-length AAG.

was excised by AAG from both single- and double-stranded DNA; only the full-length AAG exhibited such activity. The

single-turnover excision with U appeared to be very slow and exhibited kinetics that followed a linear rather than an



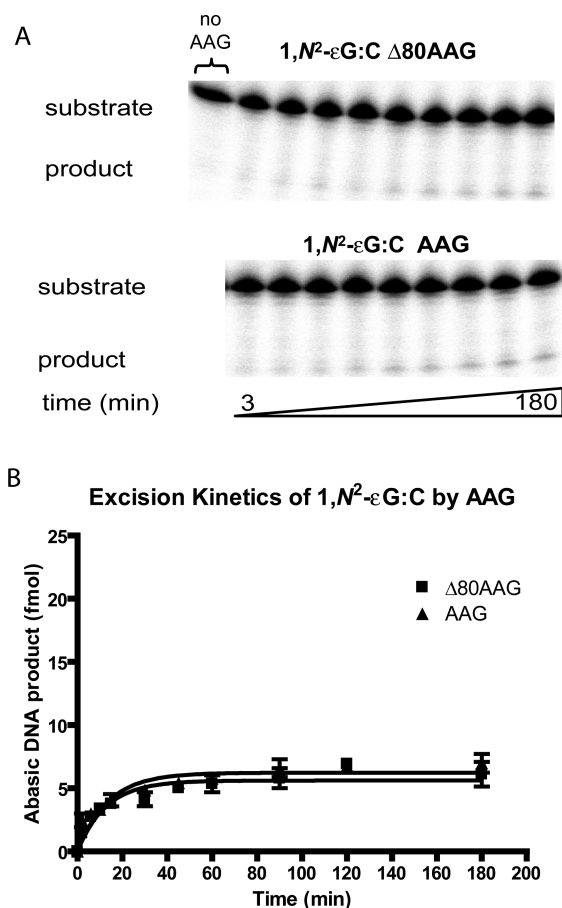


FIGURE 6: 1,N<sup>2</sup>-εG in double-stranded DNA is a substrate for both the Δ80 truncated form and the full-length AAG protein. (A) Glycosylase activity of AAG toward 1,N<sup>2</sup>-εG by Δ80AAG and full-length AAG. No AAG represents incubation without AAG for the longest time point of the assay. (B) Graphical representation of the glycosylase activity toward 1,N<sup>2</sup>-εG by (■) Δ80AAG and (▲) full-length AAG.

exponential fit, yielding initial excision rates (and also observed rate constants) of  $\sim 0.06$  fmol/min for both single- and double-stranded DNA (Table 1), which is  $\sim 7$ -fold lower than that for 1,N<sup>2</sup>-εG, whose level of saturation cleavage was only  $\sim 6\%$  (Figure 6B). Although uracil can be weakly cleaved by AAG, the alkylated m3U and e3U (deamination products of m3C and e3C, respectively) were not excised despite their significant binding to AAG. In contrast, the EMSA was not sensitive enough to detect binding of either form of AAG to substrates containing U. Notably, among the substrates tested in this study, uracil was the only substrate toward which the truncated and full-length AAG exhibited different activity.

## DISCUSSION

The human 3-methyladenine DNA glycosylase (AAG) is known to have a broad substrate specificity for damaged purines, including 3-methyladenine, 7-methylguanine, εA, and Hx (2–8). In this report, we examined substrate binding and excision kinetics of both full-length and truncated Δ80AAG, for a library of lesion-containing DNA oligonucleotides in both the single- and double-stranded form. In addition to confirming previous findings, we identified several new substrates for full-length and truncated AAG in single- and double-stranded DNA, namely, m1G (ds), Hx

(ss), 1,N<sup>2</sup>-εG (ds by Δ80AAG), and uracil (both ss and ds by full-length AAG).

Although human AAG has been primarily shown to repair lesions in double-stranded DNA, excision activity on single-stranded DNA was previously observed for εA and oxanine (40). Binding and excision of oxanine in duplex DNA appear to be independent of the opposite base; indeed, a complementary strand is not necessary as seen from the similar binding and excision efficiencies for oxanine in 62-mer single- and double-stranded DNA (40). In addition to AAG, other DNA glycosylases have also been shown to excise damaged bases from single-stranded DNA. For instance, in *E. coli*, the 3-methyladenine glycosylase (AlkA) has been shown to remove 3-methyladenine from single-stranded DNA (43), and in mammals, the bovine uracil DNA glycosylase (UDG) (44) and human SMUG1 (45) also excise uracil from single-stranded DNA substrate. In this study, we have observed AAG activity on lesion-containing single-stranded DNA. We found both εA and Hx within single-stranded DNA to be good substrates for AAG. εA was excised with similar observed rate constants in single- and double-stranded DNA, although in single-stranded DNA the initial excision rates were lower (Table 1). For Hx, it was previously shown that Hx could only be excised when paired with a base, preferably T rather than C (36, 40, 46–48), and not in single-stranded DNA, suggesting that it is the base pair instead of the damaged base alone that affects the recognition by AAG. However, to our surprise, we observed that Hx can also be repaired in single-stranded DNA, although with observed rate constants  $\sim 7$ -fold lower (initial rates  $\sim 15$ -fold lower) than those in double-stranded DNA (Table 1). Excision from the single-stranded DNA may be possible because the reduced level of base stacking and the lack of base pairing may increase the chances of the damaged bases being captured from the less rigid single-stranded structure. One might argue that the single-stranded DNA may form a secondary structure containing duplex DNA, thus allowing excision to occur. However, other than εA and Hx (and uracil to a weak extent), no other substrates were observed to be excised from single-stranded DNA, indicating that excision of lesions from single-stranded DNA may be damage-specific. A previous report showed that AAG did not bind or excise the DNA duplexes with εA or Hx paired opposite an abasic site (36), suggesting that the binding of damaged purine bases by AAG may require an opposite base or an opposite strand. However, we demonstrated catalytic activity toward εA and Hx in single-stranded DNA, although no binding of AAG to single-stranded DNA was detected by the gel shift assay.

During DNA replication and transcription, the transient single-stranded regions that arise may expose more potential sites of damage on the DNA bases; therefore, it would be beneficial to the cell if there is a mechanism for repairing damage on single-stranded DNA, especially if it is replication- or transcription-blocking. Although the advantage of base excision in single-stranded DNA is not evident, it is possible that in vivo, an abasic site or strand break may cause replication or transcription to stop. Polymerase arrest could stimulate recombination, and a stalled RNA polymerase may trigger transcription-coupled repair. Conversion of a diverse set of lesions to a uniform AP site may be a way to consistently trigger a repair–recruitment signal.



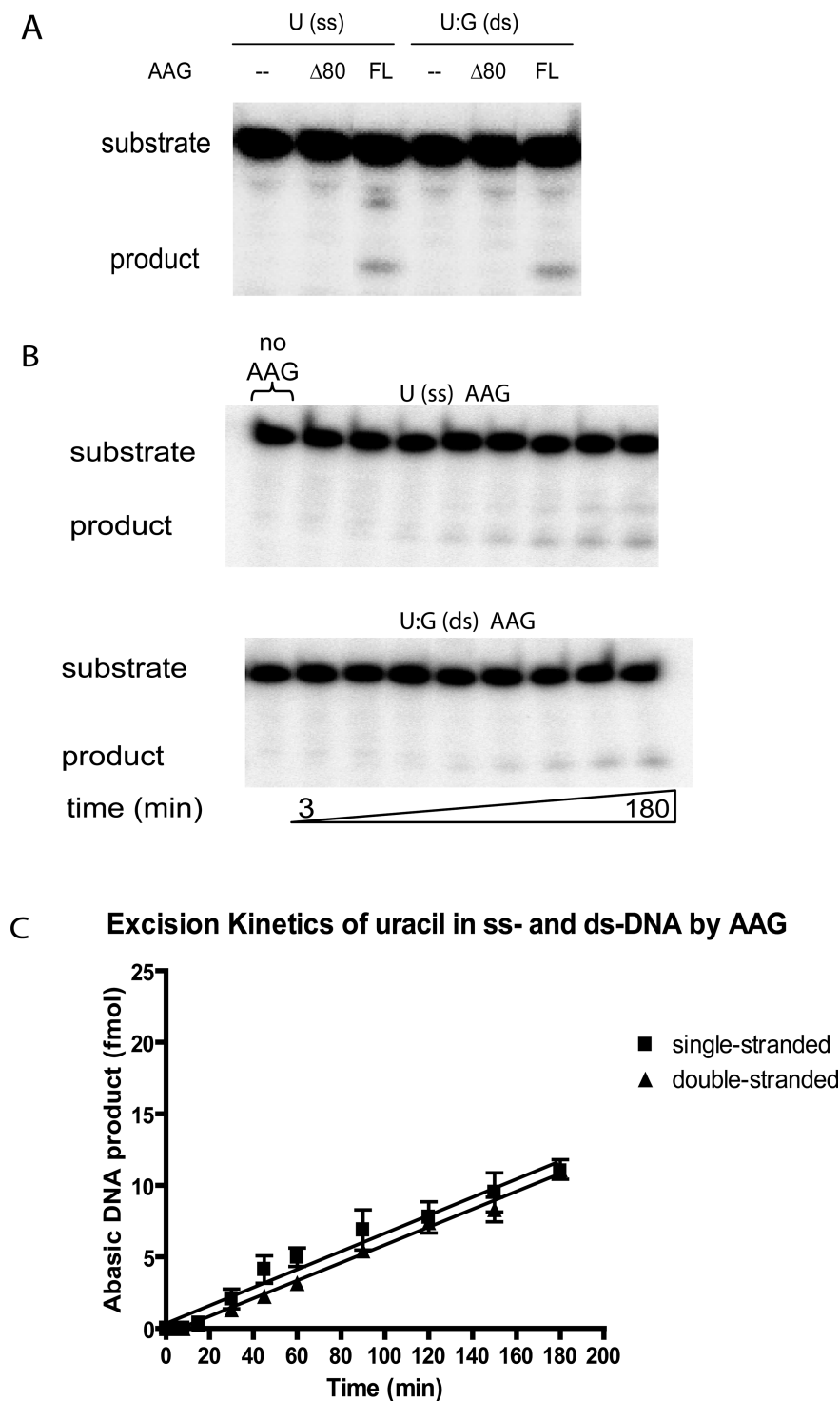


FIGURE 7: Uracil is a substrate for the full-length AAG protein in both single- and double-stranded DNA. (A) Glycosylase activity of  $\Delta 80$  vs full-length AAG toward U. (B) Glycosylase activity of full-length AAG toward U. No AAG represents incubation without AAG for the longest time point of the assay. (C) Graphical representation of the glycosylase activity toward U by full-length AAG in (■) single-stranded and (▲) double-stranded DNA.

In addition to the aforementioned  $\epsilon$ A, we have also found that AAG and AlkB share other classes of DNA damage as substrates such as EA and m1G. Formed by chloroethyl nitrosoureas that are used in cancer therapy and structurally similar to  $\epsilon$ A, ethanoadenine (EA) was recently shown to be metabolized by AlkB (22). Unlike  $\epsilon$ A whose unsaturated exocyclic ring is planar, EA's nonplanar saturated ring may give rise to less stable aromatic base stacking interactions with the active site residues of AAG, possibly leading to the poorer binding ability and less efficient repair of EA.

Guliaev et al. (35) showed that AAG was able to repair EA, but with a 65-fold lower efficiency than for  $\epsilon$ A. We, however, found an only  $\sim 4$ -fold difference in initial excision rates in this study (Table 1); this discrepancy could be possibly due to differences in sequence context, or the position of the lesion. Despite AAG's weak binding to EA, excision was efficient, with up to 30% EA being released (Figure 4C,D and Table 1). In addition to cyclic lesions (22–24), simple methylated lesions such as m1G, m3T, m1A, and m3C also interfere with normal Watson–Crick base pairing and were

all shown to be AlkB substrates (13–17). However, despite the observed binding between AAG and these lesions, excision was only seen for m1G (Figure 3A,B and Table 1). It is also worth reiterating that binding affinity clearly does not predict excision activity. For instance, AAG exhibited very weak binding to m1G (Table 1 and Figure 3), yet it was able to excise ~50% of m1G at saturation (Figure 4A,B), making m1G among the top three lesions to be excised. In fact, AAG bound to a Hx:T canonical substrate only moderately well (with a  $K_d$  of 125 nM) yet exhibited the fastest excision rate (Table 1). We observed instances in which strong binding substrates are weakly excised and vice versa. Indeed, AAG does not excise all of the substrates to which it binds. Hence, it is very difficult to point out any trends relating binding affinity and excision rates.

We questioned why AAG can cleave m1G but not the structurally analogous m1A. Some main differences between m1A and m1G include the O6 atom of m1G, which can serve as a hydrogen bond acceptor from the main chain amide of His136 in the enzyme active site, whereas m1A has an amino group at the N6 position and cannot accept the hydrogen bond for stabilization (which is how AAG discriminates against normal adenines) (9). Moreover, m1A is positively charged and lacks a 2-amino group, whereas m1G is neutral and, like guanine, has a 2-amino group that could clash with Asn169. Charge probably has little effect on the AAG-mediated excision in this case, since the positively charged m1A is not a better substrate than m1G. Perhaps the hydrogen bond between the O6 position of the m1G base and His136 enhances binding in the active site and plays a stronger role in recognition and binding than the cation– $\pi$  interaction between the positively charged m1A and the aromatic active site residues. The lack of excision of m3C and m3T was expected and may be explained by the fact that protonation of the nucleobase likely occurs at N7 or N3 of purines for AAG-catalyzed excision (11) and is more suitable for purines than for pyrimidines, eliminating the likelihood of repairing cytosine or thymine adducts.

AAG protein can exist as several alternatively spliced forms (49–52), and it has been shown that the nonconserved N-terminus does not affect the recognition and glycosylase activity for some substrates (6, 53). In a previous study, Saparbaev et al. found that both the full-length AAG and the truncated AAG lacking the first 73 amino acid residues were able to bind to 1, $N^2$ - $\epsilon$ G, but only the full-length protein was able to release it from duplex DNA (41). It was suggested that a change in the active site conformation of truncated AAG and the absence of N-terminal amino acid residues essential for  $\epsilon$ G catalysis are possible factors responsible for the inactivity of truncated AAG on  $\epsilon$ G. Here we also found 1, $N^2$ - $\epsilon$ G to be a substrate for AAG, as previously reported (26, 41). However, in our study, both the full-length protein and  $\Delta$ 80AAG excised 1, $N^2$ - $\epsilon$ G equally well, albeit weakly (Figure 6A,B and Table 1). Perhaps the possible conformational change caused by deletion of the N-terminal tail still allows the protein to bind and excise the shorter 16-mer oligonucleotides (this study) but hinders excision in the longer oligonucleotides [30–31-mer used by Saparbaev et al. (41)]. The fact that 1, $N^2$ - $\epsilon$ G is repaired by MUG (41) and AAG (Figure 6 and Table 1) (41, 54) underscores the importance of its repair for proper cellular homeostasis. In another study, Adhikari et al. found that the

N-terminal tail is required for the turnover in the Hx excision reaction (39). Their experiments using both truncated ( $\Delta$ 100) and full-length AAG showed that truncation crippled the turnover of AAG activity on Hx under multiple-turnover conditions, but not under single-turnover conditions (39). The binding experiments using SPR spectroscopy showed that the truncated AAG binds AP site-containing DNA with 6-fold higher affinity compared to Hx-containing DNA. In contrast, full-length AAG showed almost equal binding affinity toward its product as well as its substrate. Therefore, the study concluded that the N-terminus of AAG plays important role in overcoming product inhibition (39).

AAG is known to have an additional role in repairing deaminated bases such as hypoxanthine and oxanine. Uracil arises as a deamination product of cytosine, or it can be misincorporated opposite A from the dNTP pool during DNA synthesis. Like all deaminated base lesions, uracil is promutagenic, and efficient repair of this lesion is accomplished by base excision involving uracil DNA glycosylases (UDGs), comprised of four families thus far (45, 55). In this study, we have found that the full-length AAG (and not  $\Delta$ 80AAG) can excise uracil, a pyrimidine, to a limited extent with slow excision kinetics, in single- or double-stranded DNA when paired with G (Figure 7A–C and Table 1). Single-stranded activity was also observed here, similar to that in the deaminated bases hypoxanthine (Figure 5D–F and Table 1) and oxanine (40). The UNG2 and SMUG1 glycosylases exhibit initial excision rates of approximately 10% per minute ( $0.1 \text{ min}^{-1}$ ) for a 146-mer oligonucleotide, with the removal being almost complete by 15 min (56); for pyrimidines in addition to uracil, the MUG uracil DNA glycosylase excises  $\epsilon$ C:G, U:G, and T:G mismatches with rate constants of ~0.2, 0.04, and  $2.5 \times 10^{-6} \text{ s}^{-1}$ , respectively (57). Thus, compared to the rates of other uracil glycosylases, AAG activity toward uracil ( $\sim 6 \times 10^{-4} \text{ min}^{-1}$ ) is relatively weak and may not account for significant uracil removal in vivo.

According to previous structural and biochemical studies, AAG has been proposed to remove damaged purines using the general acid–base catalysis reaction mechanism (58). In this mechanism, the first step is the leaving group activation in which the damaged purine is protonated at N7 by a water molecule from the bulk solvent. This step, which is coupled to nucleophile activation and its approach, destabilizes the glycosidic bond, resulting in removal of the damaged base and formation of an abasic site. Assuming that the site of protonation is conserved in AAG, one can propose that AAG effectively protonates all purines and might fail to effectively protonate the damaged pyrimidines because of its unfavorable binding stereochemistry in the active site. However, the removal of the uracil base has been proposed to be different from that of the general acid–base catalysis mechanism and is known to be removed in its anionic form (58). Various studies on UDGs have shown that these enzymes remove uracil through the effective stabilization of its free anionic form (58). The activity of full-length AAG on uracil can be explained on the basis of the hypothesis that similar to UDGs, the active site of AAG might also stabilize the anionic form of uracil base, thereby resulting in its removal.

In conclusion, we report significant overlap in substrate specificity between AAG and other repair enzymes such as AlkB, MUG, and UDG. As a genotoxic and mutagenic

lesion, m1G was known to be a substrate repaired efficiently by the direct reversal protein AlkB, and we now find that it is a good AAG substrate. It would seem advantageous to the cell to have backup DNA repair systems for eliminating this lesion in the event that one system is unavailable. Evaluation of the mutagenic and genotoxic activities of m1G in AAG-proficient and AAG-deficient cell lines is a priority based upon this study. As a damaged lesion from the environment and from lipid peroxidation byproducts, 1,N<sup>2</sup>-εG is also a shared substrate between MUG and AAG. Although both truncated and full-length AAG exhibited similar glycosylase activity toward most substrates in this study, it was shown by another study that the N-terminal domain was essential in the excision of 1,N<sup>2</sup>-εG. However, we did find that the truncated and full-length AAG protein exhibited different activity toward uracil, highlighting the significance of the N-terminus in the glycosylase activity of AAG. Moreover, our results for AAG activity on εA- and Hx-containing single-stranded DNA may underscore the significance of single-stranded DNA repair, in which other repair proteins such as photolyase and AlkB are also involved.

## ACKNOWLEDGMENT

We thank Jennifer Calvo and Lisiane Meira for important comments on the manuscript. We also thank Carmelo Rizzo and Lawrence Marnett for the synthesis of the oligonucleotides containing 1,N<sup>2</sup>-εG and MIG.

## REFERENCES

- Friedberg, E. C., Walker, G. C., Siede, W., Wood, R. D., Schultz, R. A., and Ellenberger, T. (2006) *DNA Repair and Mutagenesis*, 2nd ed., ASM Press, Washington, DC.
- Engelward, B. P., Weeda, G., Wyatt, M. D., Broekhof, J. L., de Wit, J., Donker, I., Allan, J. M., Gold, B., Hoeijmakers, J. H., and Samson, L. D. (1997) Base excision repair deficient mice lacking the Aag alkyladenine DNA glycosylase. *Proc. Natl. Acad. Sci. U.S.A.* **94**, 13087–13092.
- Gallagher, P. E., and Brent, T. P. (1982) Partial purification and characterization of 3-methyladenine-DNA glycosylase from human placenta. *Biochemistry* **21**, 6404–6409.
- Hang, B., Singer, B., Margison, G. P., and Elder, R. H. (1997) Targeted deletion of alkylpurine-DNA-N-glycosylase in mice eliminates repair of 1,N<sup>6</sup>-ethenoadenine and hypoxanthine but not of 3,N<sup>4</sup>-ethenocytosine or 8-oxoguanine. *Proc. Natl. Acad. Sci. U.S.A.* **94**, 12869–12874.
- Miao, F., Bouziane, M., and O'Connor, T. R. (1998) Interaction of the recombinant human methylpurine-DNA glycosylase (MPG protein) with oligodeoxyribonucleotides containing either hypoxanthine or abasic sites. *Nucleic Acids Res.* **26**, 4034–4041.
- O'Connor, T. R. (1993) Purification and characterization of human 3-methyladenine-DNA glycosylase. *Nucleic Acids Res.* **21**, 5561–5569.
- Saparbaev, M., and Laval, J. (1994) Excision of hypoxanthine from DNA containing dIMP residues by the *Escherichia coli*, yeast, rat, and human alkylpurine DNA glycosylases. *Proc. Natl. Acad. Sci. U.S.A.* **91**, 5873–5877.
- Singer, B., Antoccia, A., Basu, A. K., Dosanjh, M. K., Fraenkel-Conrat, H., Gallagher, P. E., Kusmierek, J. T., Qiu, Z. H., and Rydberg, B. (1992) Both purified human 1,N<sup>6</sup>-ethenoadenine-binding protein and purified human 3-methyladenine-DNA glycosylase act on 1,N<sup>6</sup>-ethenoadenine and 3-methyladenine. *Proc. Natl. Acad. Sci. U.S.A.* **89**, 9386–9390.
- Lau, A. Y., Wyatt, M. D., Glassner, B. J., Samson, L. D., and Ellenberger, T. (2000) Molecular basis for discriminating between normal and damaged bases by the human alkyladenine glycosylase, AAG. *Proc. Natl. Acad. Sci. U.S.A.* **97**, 13573–13578.
- Lau, A. Y., Scharer, O. D., Samson, L., Verdine, G. L., and Ellenberger, T. (1998) Crystal structure of a human alkylbase-DNA repair enzyme complexed to DNA: Mechanisms for nucleotide flipping and base excision. *Cell* **95**, 249–258.
- O'Brien, P. J., and Ellenberger, T. (2003) Human alkyladenine DNA glycosylase uses acid-base catalysis for selective excision of damaged purines. *Biochemistry* **42**, 12418–12429.
- O'Brien, P. J., and Ellenberger, T. (2004) Dissecting the broad substrate specificity of human 3-methyladenine-DNA glycosylase. *J. Biol. Chem.* **279**, 9750–9757.
- Trewhick, S. C., Henshaw, T. F., Hausinger, R. P., Lindahl, T., and Sedgwick, B. (2002) Oxidative demethylation by *Escherichia coli* AlkB directly reverts DNA base damage. *Nature* **419**, 174–178.
- Falnes, P. O., Johansen, R. F., and Seeberg, E. (2002) AlkB-mediated oxidative demethylation reverses DNA damage in *Escherichia coli*. *Nature* **419**, 178–182.
- Delaney, J. C., and Essigmann, J. M. (2004) Mutagenesis, genotoxicity, and repair of 1-methyladenine, 3-alkylcytosines, 1-methylguanine, and 3-methylthymine in alkB *Escherichia coli*. *Proc. Natl. Acad. Sci. U.S.A.* **101**, 14051–14056.
- Falnes, P. O. (2004) Repair of 3-methylthymine and 1-methylguanine lesions by bacterial and human AlkB proteins. *Nucleic Acids Res.* **32**, 6260–6267.
- Koivisto, P., Robins, P., Lindahl, T., and Sedgwick, B. (2004) Demethylation of 3-methylthymine in DNA by bacterial and human DNA dioxygenases. *J. Biol. Chem.* **279**, 40470–40474.
- Aas, P. A., Otterlei, M., Falnes, P. O., Vagbo, C. B., Skorpen, F., Akbari, M., Sundheim, O., Bjoras, M., Slupphaug, G., Seeberg, E., and Krokan, H. E. (2003) Human and bacterial oxidative demethylases repair alkylation damage in both RNA and DNA. *Nature* **421**, 859–863.
- Falnes, P. O., Bjoras, M., Aas, P. A., Sundheim, O., and Seeberg, E. (2004) Substrate specificities of bacterial and human AlkB proteins. *Nucleic Acids Res.* **32**, 3456–3461.
- Ougland, R., Zhang, C. M., Liiv, A., Johansen, R. F., Seeberg, E., Hou, Y. M., Remme, J., and Falnes, P. O. (2004) AlkB restores the biological function of mRNA and tRNA inactivated by chemical methylation. *Mol. Cell* **16**, 107–116.
- Westbye, M. P., Feyzi, E., Aas, P. A., Vagbo, C. B., Talstad, V. A., Kavli, B., Hagen, L., Sundheim, O., Akbari, M., Liabakk, N. B., Slupphaug, G., Otterlei, M., and Krokan, H. E. (2008) Human AlkB homolog 1 is a mitochondrial protein that demethylates 3-methylcytosine in DNA and RNA. *J. Biol. Chem.* **283**, 25046–25056.
- Frick, L. E., Delaney, J. C., Wong, C., Drennan, C. L., and Essigmann, J. M. (2007) Alleviation of 1,N<sup>6</sup>-ethenoadenine genotoxicity by the *Escherichia coli* adaptive response protein AlkB. *Proc. Natl. Acad. Sci. U.S.A.* **104**, 755–760.
- Delaney, J. C., Smeester, L., Wong, C., Frick, L. E., Taghizadeh, K., Wishnok, J. S., Drennan, C. L., Samson, L. D., and Essigmann, J. M. (2005) AlkB reverses etheno DNA lesions caused by lipid oxidation in vitro and in vivo. *Nat. Struct. Mol. Biol.* **12**, 855–860.
- Mishina, Y., Yang, C. G., and He, C. (2005) Direct repair of the exocyclic DNA adduct 1,N<sup>6</sup>-ethenoadenine by the DNA repair AlkB proteins. *J. Am. Chem. Soc.* **127**, 14594–14595.
- Ringvoll, J., Moen, M. N., Nordstrand, L. M., Meira, L. B., Pang, B., Bekkelund, A., Dedon, P. C., Bjelland, S., Samson, L. D., Falnes, P. O., and Klungland, A. (2008) AlkB homologue 2-mediated repair of ethenoadenine lesions in mammalian DNA. *Cancer Res.* **68**, 4142–4149.
- Dosanjh, M. K., Chenna, A., Kim, E., Fraenkel-Conrat, H., Samson, L., and Singer, B. (1994) All four known cyclic adducts formed in DNA by the vinyl chloride metabolite chloroacetaldehyde are released by a human DNA glycosylase. *Proc. Natl. Acad. Sci. U.S.A.* **91**, 1024–1028.
- el Ghissassi, F., Barbin, A., and Bartsch, H. (1998) Metabolic activation of vinyl chloride by rat liver microsomes: Low-dose kinetics and involvement of cytochrome P450 2E1. *Biochem. Pharmacol.* **55**, 1445–1452.
- Guengerich, F. P. (1992) Roles of the vinyl chloride oxidation products 1-chlorooxirane and 2-chloroacetaldehyde in the in vitro formation of etheno adducts of nucleic acid bases [corrected]. *Chem. Res. Toxicol.* **5**, 2–5.
- Guengerich, F. P., Crawford, W. M., Jr., and Watanabe, P. G. (1979) Activation of vinyl chloride to covalently bound metabolites: Roles of 2-chloroethylene oxide and 2-chloroacetaldehyde. *Biochemistry* **18**, 5177–5182.
- Guengerich, F. P., Persmark, M., and Humphreys, W. G. (1993) Formation of 1,N<sup>2</sup>- and N<sup>2</sup>,3-ethenoguanine from 2-haloalkoxiranes: Isotopic labeling studies and isolation of a hemiaminal derivative of N<sup>2</sup>-(2-oxoethyl)guanine. *Chem. Res. Toxicol.* **6**, 635–648.



31. Kusmierek, J. T., and Singer, B. (1982) Chloroacetaldehyde-treated ribo- and deoxyribopolynucleotides. 1. Reaction products. *Biochemistry* 21, 5717–5722.
32. Kusmierek, J. T., and Singer, B. (1992) 1,N2-Ethenodeoxyguanosine: Properties and formation in chloroacetaldehyde-treated polynucleotides and DNA. *Chem. Res. Toxicol.* 5, 634–638.
33. Leonard, N. J. (1984) Etheno-substituted nucleotides and coenzymes: Fluorescence and biological activity. *CRC Crit. Rev. Biochem.* 15, 125–199.
34. Ludlum, D. B. (1990) DNA alkylation by the haloethylnitrosoureas: Nature of modifications produced and their enzymatic repair or removal. *Mutat. Res.* 233, 117–126.
35. Guliaev, A. B., Hang, B., and Singer, B. (2002) Structural insights by molecular dynamics simulations into differential repair efficiency for ethano-A versus etheno-A adducts by the human alkylpurine-DNA N-glycosylase. *Nucleic Acids Res.* 30, 3778–3787.
36. Abner, C. W., Lau, A. Y., Ellenberger, T., and Bloom, L. B. (2001) Base excision and DNA binding activities of human alkyladenine DNA glycosylase are sensitive to the base paired with a lesion. *J. Biol. Chem.* 276, 13379–13387.
37. Goodenough, A. K., Kozekov, I. D., Zang, H., Choi, J. Y., Guengerich, F. P., Harris, T. M., and Rizzo, C. J. (2005) Site specific synthesis and polymerase bypass of oligonucleotides containing a 6-hydroxy-3,5,6,7-tetrahydro-9H-imidazo[1,2-a]purin-9-one base, an intermediate in the formation of 1,N2-etheno-2'-deoxyguanosine. *Chem. Res. Toxicol.* 18, 1701–1714.
38. Wang, H., Kozekov, I. D., Kozekova, A., Tamura, P. J., Marnett, L. J., Harris, T. M., and Rizzo, C. J. (2006) Site-specific synthesis of oligonucleotides containing malondialdehyde adducts of deoxyguanosine and deoxyadenosine via a postsynthetic modification strategy. *Chem. Res. Toxicol.* 19, 1467–1474.
39. Adhikari, S., Uren, A., and Roy, R. (2007) N-Terminal extension of N-methylpurine DNA glycosylase is required for turnover in hypoxanthine excision reaction. *J. Biol. Chem.* 282, 30078–30084.
40. Hitchcock, T. M., Dong, L., Connor, E. E., Meira, L. B., Samson, L. D., Wyatt, M. D., and Cao, W. (2004) Oxanine DNA glycosylase activity from mammalian alkyladenine glycosylase. *J. Biol. Chem.* 279, 38177–38183.
41. Saparbaev, M., Langouet, S., Privezentzev, C. V., Guengerich, F. P., Cai, H., Elder, R. H., and Laval, J. (2002) 1,N(2)-Ethenoguanine, a mutagenic DNA adduct, is a primary substrate of *Escherichia coli* mismatch-specific uracil-DNA glycosylase and human alkylpurine-DNA-N-glycosylase. *J. Biol. Chem.* 277, 26987–26993.
42. Wuenschell, G. E., O'Connor, T. R., and Termini, J. (2003) Stability, miscoding potential, and repair of 2'-deoxyxanthosine in DNA: Implications for nitric oxide-induced mutagenesis. *Biochemistry* 42, 3608–3616.
43. Bjelland, S., and Seeberg, E. (1996) Different efficiencies of the Tag and AlkA DNA glycosylases from *Escherichia coli* in the removal of 3-methyladenine from single-stranded DNA. *FEBS Lett.* 397, 127–129.
44. Eftedal, I., Guddal, P. H., Slupphaug, G., Volden, G., and Krokan, H. E. (1993) Consensus sequences for good and poor removal of uracil from double stranded DNA by uracil-DNA glycosylase. *Nucleic Acids Res.* 21, 2095–2101.
45. Haushalter, K. A., Todd Stukenberg, M. W., Kirschner, M. W., and Verdine, G. L. (1999) Identification of a new uracil-DNA glycosylase family by expression cloning using synthetic inhibitors. *Curr. Biol.* 9, 174–185.
46. Dianov, G., and Lindahl, T. (1991) Preferential recognition of I•T base-pairs in the initiation of excision-repair by hypoxanthine-DNA glycosylase. *Nucleic Acids Res.* 19, 3829–3833.
47. Saparbaev, M., Mani, J. C., and Laval, J. (2000) Interactions of the human, rat, *Saccharomyces cerevisiae* and *Escherichia coli* 3-methyladenine-DNA glycosylases with DNA containing dIMP residues. *Nucleic Acids Res.* 28, 1332–1339.
48. Wyatt, M. D., and Samson, L. D. (2000) Influence of DNA structure on hypoxanthine and 1,N(6)-ethenoadenine removal by murine 3-methyladenine DNA glycosylase. *Carcinogenesis* 21, 901–908.
49. Chakravarti, D., Ibeanu, G. C., Tano, K., and Mitra, S. (1991) Cloning and expression in *Escherichia coli* of a human cDNA encoding the DNA repair protein N-methylpurine-DNA glycosylase. *J. Biol. Chem.* 266, 15710–15715.
50. O'Connor, T. R., and Laval, J. (1991) Human cDNA expressing a functional DNA glycosylase excising 3-methyladenine and 7-methylguanine. *Biochem. Biophys. Res. Commun.* 176, 1170–1177.
51. Pendlebury, A., Frayling, I. M., Santibanez Koref, M. F., Margison, G. P., and Rafferty, J. A. (1994) Evidence for the simultaneous expression of alternatively spliced alkylpurine N-glycosylase transcripts in human tissues and cells. *Carcinogenesis* 15, 2957–2960.
52. Samson, L., Derfler, B., Boosalis, M., and Call, K. (1991) Cloning and characterization of a 3-methyladenine DNA glycosylase cDNA from human cells whose gene maps to chromosome 16. *Proc. Natl. Acad. Sci. U.S.A.* 88, 9127–9131.
53. Roy, R., Biswas, T., Hazra, T. K., Roy, G., Grabowski, D. T., Izumi, T., Srinivasan, G., and Mitra, S. (1998) Specific interaction of wild-type and truncated mouse N-methylpurine-DNA glycosylase with ethenoadenine-containing DNA. *Biochemistry* 37, 580–589.
54. Elder, R. H., Jansen, J. G., Weeks, R. J., Willington, M. A., Deans, B., Watson, A. J., Mynett, K. J., Bailey, J. A., Cooper, D. P., Rafferty, J. A., Heeran, M. C., Wijnhoven, S. W., van Zeeland, A. A., and Margison, G. P. (1998) Alkylpurine-DNA-N-glycosylase knockout mice show increased susceptibility to induction of mutations by methyl methanesulfonate. *Mol. Cell. Biol.* 18, 5828–5837.
55. Pearl, L. H. (2000) Structure and function in the uracil-DNA glycosylase superfamily. *Mutat. Res.* 460, 165–181.
56. Nilsen, H., Lindahl, T., and Verreault, A. (2002) DNA base excision repair of uracil residues in reconstituted nucleosome core particles. *EMBO J.* 21, 5943–5952.
57. O'Neill, R. J., Vorob'eva, O. V., Shahbakhti, H., Zmuda, E., Bhagwat, A. S., and Baldwin, G. S. (2003) Mismatch uracil glycosylase from *Escherichia coli*: A general mismatch or a specific DNA glycosylase? *J. Biol. Chem.* 278, 20526–20532.
58. Berti, P. J., and McCann, J. A. (2006) Toward a detailed understanding of base excision repair enzymes: Transition state and mechanistic analyses of N-glycoside hydrolysis and N-glycoside transfer. *Chem. Rev.* 106, 506–555.

BI8018898